

Short-Packet Communications for MIMO NOMA Systems over Nakagami- m Fading: BLER and Minimum Blocklength Analysis

Duc-Dung Tran, *Student Member, IEEE*, Shree Krishna Sharma, *Senior Member, IEEE*, Symeon Chatzinotas, *Senior Member, IEEE*, Isaac Woungang, *Senior Member, IEEE*, and Björn Ottersten, *Fellow, IEEE*

Abstract—Recently, ultra-reliable and low-latency communications (URLLC) using short-packets has been proposed to fulfill the stringent requirements regarding reliability and latency of emerging applications in 5G and beyond networks. In addition, multiple-input multiple-output non-orthogonal multiple access (MIMO NOMA) is a potential candidate to improve the spectral efficiency, reliability, latency, and connectivity of wireless systems. In this paper, we investigate short-packet communications (SPC) in a multiuser downlink MIMO NOMA system over Nakagami- m fading, and propose two antenna-user selection methods considering two clusters of users having different priority levels. In contrast to the widely-used long data-packet assumption, the SPC analysis requires the redesign of the communication protocols and novel performance metrics. Given this context, we analyze the SPC performance of MIMO NOMA systems using the average block error rate (BLER) and minimum blocklength, instead of the conventional metrics such as ergodic capacity and outage capacity. More specifically, to characterize the system performance regarding SPC, asymptotic (in the high signal-to-noise ratio regime) and approximate closed-form expressions of the average BLER at the users are derived. Based on the asymptotic behavior of the average BLER, an analysis of the diversity order, minimum blocklength, and optimal power allocation is carried out. The achieved results show that MIMO NOMA can serve multiple users simultaneously using a smaller blocklength compared with MIMO OMA, thus demonstrating the benefits of MIMO NOMA for SPC in minimizing the transmission latency. Furthermore, our results indicate that the proposed methods not only improve the BLER performance but also guarantee full diversity gains for the respective users.

Index Terms—Block error rate, MIMO, minimum blocklength, non-orthogonal multiple access, short-packet communications.

I. INTRODUCTION

Ultra-reliable and low-latency communications (URLLC) has recently been considered as a promising technology for the 5th generation (5G) and beyond wireless networks to support novel applications with unprecedented requirements of reliability and latency [1–3]. Furthermore, it is a potential solution for mission-critical Internet of Things (IoT) applications such as industrial automation, remote surgery, and vehicle-to-everything (V2X) communications, which require high reliability and low latency [4]. URLLC systems should be designed

to meet the requirements of high reliability (99.999%) and low latency (1 ms) [5]. To achieve such stringent requirements, a new transmission approach, i.e., short-packet communications (SPC), could be a promising solution. This is different from the traditional analytic methods designed to target Shannon’s channel capacity using long data-packets, which are no longer suitable for low latency systems [5]. To characterize the performance of SPC, new performance metrics including block error rate (BLER) and overhead ratio (i.e., ratio of pilots to the information payload), have been introduced in the literature [6–8].

Besides, non-orthogonal multiple access (NOMA) has recently emerged as a promising technology to improve the spectral efficiency and user fairness for wireless networks [9, 10]. In contrast to the orthogonal multiple access (OMA) which utilizes orthogonal resources (e.g., time and frequency) to support multiple users, this technique can serve them at the same time/frequency/code by using the power domain and effective interference management methods, such as successive interference cancellation (SIC) [9]. Therefore, NOMA can more effectively support massive connectivity and further improve the reliability and latency for wireless systems [11, 12]. With its potential advantages, NOMA standardization has been recently studied in the 3rd Generation Partnership Project (3GPP) frameworks [13–15] including the 3GPP Release 16 [15]. Also, the latest trend is to employ NOMA in the uplink due to the emergence of IoT and machine-type communication systems [3, 15, 16]. Thus, NOMA and its variations are expected to be employed in various 5G and beyond application scenarios [12, 17, 18].

In addition, the combination of NOMA and multiple-input multiple-output (MIMO) systems (so-called MIMO NOMA), which can significantly enhance the spectral efficiency and performance of NOMA systems, has also been investigated in recent years [19, 20]. The ergodic capacity analysis of MIMO NOMA systems has been considered in [21], where the authors have proved the superiority of MIMO NOMA over MIMO OMA in terms of capacity. Furthermore, a transmit antenna selection (TAS) scheme has been proposed to reduce the complexity and improve the performance gain of MIMO NOMA systems [22, 23]. It is noteworthy that the above works on MIMO NOMA have been conducted under the assumption of long data-packet transmissions, which is no longer applicable for emerging URLLC applications with short data-packets in 5G and beyond networks [3–5].

This work was supported by the National Research Fund (FNR), Luxembourg under the CORE Project 5G-Sky.

D.-D. Tran, S. K. Sharma, S. Chatzinotas, and B. Ottersten are with Interdisciplinary Center for Security, Reliability and Trust (SnT), University of Luxembourg, 4365 Esch-sur-Alzette, Luxembourg (e-mail: duc.tran@uni.lu; shree.sharma@uni.lu; Symeon.Chatzinotas@uni.lu; bjorn.ottersten@uni.lu).

I. Woungang is with the Department of Computer Science, Ryerson University, Toronto, ON M5B 2K3, Canada (email: iwoungan@ryerson.ca).

To overcome this challenge, in this paper, we propose to utilize SPC for MIMO NOMA systems to improve the reliability and latency as well as enhance the spectral efficiency and connectivity for wireless systems. Herein, suitable performance metrics for SPC including average BLER and minimum blocklength, are utilized instead of the conventional ones such as ergodic capacity and outage capacity.

A. Related Works

Recently, there have been a few works on SPC in NOMA systems, which is considered as a promising solution to enhance the reliability, latency, and connectivity for wireless networks [24–29]. In particular, in [24], a two-user NOMA system with short-packets over Rayleigh fading channels was considered, in which the average BLER at users is derived to evaluate the system performance. In [25], the BLER performance of a NOMA system was addressed, where stochastic geometry and Nakagami- m fading channels are considered. In [26], X. Lai *et al.* analyzed the performance of a cooperative NOMA SPC system over Rayleigh fading channels. However, the works [24–26] only considered single-input single-output (SISO) systems.

To exploit the benefits of multiple antennas in improving the reliability and reducing the latency for SPC in NOMA systems, the work in [27] investigated a multiple-input single-output (MISO) scheme to evaluate the outage performance of a URLLC NOMA system with wireless power transfer. In [28], MIMO NOMA for URLLC systems was considered to enhance the reliability and latency performance of the system. In this regard, a closed-form upper bound for the delay target violation probability was derived in [28] to identify the sufficient and necessary condition for the optimal transmit power. However, the analysis of average BLER and minimum blocklength was not considered in [28]. The work in both [27] and [28] investigated a scenario where an N -antenna base station (BS) provides services to N pairs of NOMA users, in which each pair of users is served by a distinct single transmit antenna. In contrast to this scenario, in [29], the combination of transmit antennas to serve a pair of users was examined in order to enhance the BLER performance of short-packet NOMA systems by utilizing the maximum ratio transmission (MRT), in which only the MISO scenario was considered.

Although MRT can significantly improve the system performance by combining all transmit antennas for transmission, it leads to high complexity of the signal processing and feedback overhead [30]. Against this context, TAS has been proposed as a low-complexity and power-efficient solution for multi-antenna transmitters to enhance the performance of NOMA systems by selecting a best transmit antenna for transmission that maximizes the signal-to-noise ratio (SNR) at the receiver side [23, 31]. Nevertheless, the short-packet transmission in MIMO NOMA systems considering the TAS solution, average BLER, and minimum blocklength has not yet been analyzed. Furthermore, it is noted that most of these existing studies [24–29] only investigated Rayleigh fading channels. Research on SPC for MIMO NOMA systems applying TAS for the transmitter, selection combining (SC) and maximal ratio combining (MRC) for the receiver, over a generic fading channel,

i.e., Nakagami- m , to improve the system performance more effectively and bring more general insights of the system behavior has not yet been conducted, and thus is the focus of this paper.

B. Contributions

In contrast to the existing related works, in this paper, we propose a new framework to analyze the system performance of utilizing SPC in a NOMA network, in which MIMO and Nakagami- m distribution are considered. Most existing works on NOMA are conducted under the assumption that NOMA is carried out based on the difference in users' channel conditions [9–11, 18–29]. More precisely, in a two-user downlink NOMA system, a BS transmits information to the users by superimposing users' messages with different transmit power levels [9]. The user having worse channel quality is allocated with the higher power level compared with the user having a better channel condition. However, in practice, users may have similar channel conditions but require different quality of service (QoS) as discussed in [32–34]. For example, some users may need to be served faster with low targeted data-rate, i.e., incident alerts, while some users can be served with the best effort, i.e., downloading of multimedia files [33]. In such a heterogeneous scenario, NOMA scheme becomes advantageous as compared to the conventional OMA as it can concurrently serve users having different QoS priorities with the same resources (time/frequency/code).

Given this context, we examine a scenario, in which a BS communicates with two user clusters having different priority levels over Nakagami- m fading channels, where the BS and all users are equipped with multiple antennas. Note that Nakagami- m is described as a general distribution that can include the well-known Rayleigh and Rician distributions. To perform NOMA, user pairing is employed as discussed in [35–37] to reduce the strong co-channel interference in NOMA systems. Furthermore, different MIMO schemes are investigated to exploit the benefits of multiple antennas. Particularly, at the BS, TAS is utilized to select the best transmit antenna for transmission that maximizes the post-processed SNR at the receiver [23, 31]. Besides, at the user-side, two different diversity techniques are investigated: 1) SC, which selects the best received signal branch for further processing; and 2) MRC, which combines all the received signal branches from receive antennas to maximize the output SNR. The main contributions of this paper are summarized as follows:

- Firstly, we propose a novel framework to analyze the performance of an SPC-based NOMA system, where MIMO transmission and Nakagami- m fading are considered. To achieve a general insight into the system behavior, we investigate two different cases of applying MIMO schemes for the transmitter and receiver sides including TAS/SC and TAS/MRC. Moreover, we investigate two antenna-user selection methods, namely high-priority cluster selection (HCS) and low-priority cluster selection (LCS), to design the effective communication protocols for SPC in a MIMO NOMA system.
- Secondly, we derive closed-form expressions for the average BLER of users in all considered cases. It should

TABLE I
MAIN NOTATIONS AND SYMBOLS

Notation	Description
$ \cdot $ and $\ \cdot\ $	The absolute value and the Euclidean norm
$\mathcal{CN}(0, N_0)$	A scalar complex Gaussian distribution with zero mean and variance N_0
$Q(x)$	The Gaussian Q-function
$Ei(x)$	The exponential integral function
$\Gamma(x, t)$	The lower incomplete Gamma function
γ_0	Average transmit signal-to-noise ratio (SNR)
K_S and K_A	Number of antennas at base station and user A
n_A	Number of information bits for user A
N_A	Blocklength for user A
α_A	Power allocation coefficient for user A
D_A	Diversity order at user A
$\bar{\epsilon}_A$	Average BLER at user A

be noted that this work analyzes the performance in terms of average BLER, which is more suitable for SPC than widely-used performance metrics such as ergodic capacity and outage capacity [5, 6].

- Thirdly, we derive asymptotic expressions for the average BLER in the high SNR regime and carry out an analysis of diversity order, minimum blocklength and optimal power allocation for SPC-based MIMO NOMA system based on the asymptotic average BLER.
- Finally, we perform the blocklength comparison between MIMO NOMA and MIMO OMA systems to clarify the superiority of MIMO NOMA compared to MIMO OMA in terms of low-latency transmission when considering SPC.

C. Paper Structure and Notations

The remainder of the paper is organized as follows. Section II depicts in detail the system model and the proposed schemes. Section III presents the performance analysis in terms of average BLER for the investigated scenarios. Section IV describes an analysis of the asymptotic average BLER, diversity order, optimal power allocation, and minimum blocklength. Section V presents the numerical results. Finally, Section VI concludes this paper. For clarity, we provide a summary of main notations and symbols used in this paper in Table I.

II. SYSTEM MODEL

In this paper, the SPC in a multiuser downlink MIMO NOMA system over Nakagami- m fading channels is considered, as depicted in Fig. 1. The network consists of one base station (BS), denoted by S , two clusters of users, denoted by $H = \{H_1, \dots, H_I\}$ and $L = \{L_1, \dots, L_J\}$. In addition, the BS and the users in both clusters H and L are equipped with K_S , K_H , and K_L antennas, respectively. As reported earlier in Section I, it is assumed that the users' QoS requirements are taken into account in the design of the MIMO NOMA transmission in SPC instead of their channel conditions. More precisely, we consider the scenario where the users in clusters H and L are treated as high-priority and low-priority ones, respectively. Furthermore, the users are paired to perform NOMA with the purpose of decreasing the strong co-channel

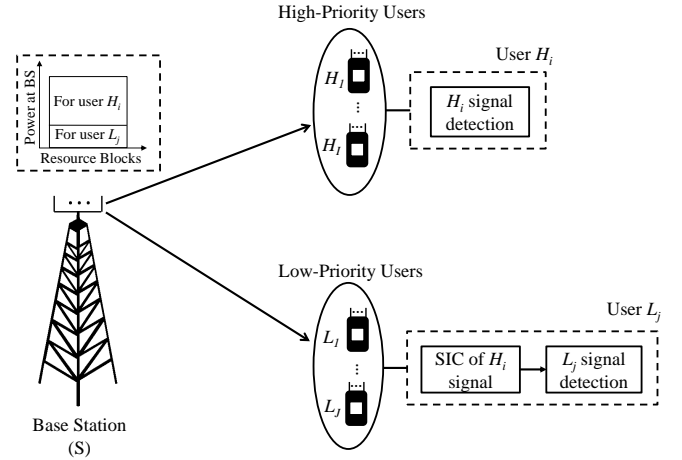


Fig. 1. Model of a MIMO NOMA system under SPC over Nakagami- m fading.

interference in NOMA systems [35–37]. Specifically, each user pair consists of two users having different priorities selected from both the clusters H and L . Moreover, as mentioned earlier in Section I, to exploit the benefits of multiple antennas, we consider the scenario where TAS is employed at the BS S whereas SC or MRC is utilized at the users' side (i.e., TAS/SC or TAS/MRC).

A. Antenna and User Selection

In this subsection, we present the proposed solutions of selecting antennas and users. As stated earlier, the user pairing is utilized for designing the MIMO NOMA. Specifically, the best user in each cluster is selected to perform NOMA based on the channel gains of the link from BS S to the users. Furthermore, we investigate two different antenna-user selection methods, i.e., HCS and LCS, which aim to improve the performance for the users selected from clusters H and L , respectively. It is noted that this selection process can be carried out prior to information transmission through a suitable signaling and channel state information (CSI) estimation method [23, 31]. In addition, as in [19, 22, 23], the required CSI for each method is assumed to be available.

1) *HCS Method*: Since the users in cluster H has higher priority than those in cluster L , this method focuses on improving the performance of the selected user in cluster H . In particular, HCS method aims to jointly select a transmit antenna and a user in cluster H to maximize the channel power gain of the link from the BS S to the selected user.

For the TAS/SC scheme, the indices of selected transmit antenna, \hat{k} , user and receive antenna selected from cluster H , \hat{i} and \hat{r}_H , are given by [30, 34]

$$(\hat{k}, \hat{i}, \hat{r}_H) = \arg \max_{1 \leq k \leq K_S, 1 \leq i \leq I, 1 \leq r \leq K_H} \left\{ |h_{S_k H_{i,r}}|^2 \right\}, \quad (1)$$

and the indices of user and receive antenna selected from cluster L , \hat{j} and \hat{r}_L , are expressed as

$$(\hat{j}, \hat{r}_L) = \arg \max_{1 \leq j \leq J, 1 \leq r \leq K_L} \left\{ |h_{S_k L_{j,r}}|^2 \right\}, \quad (2)$$

where $h_{S_k U_{m,n}}$ ($U \in \{H, L\}$) denotes the channel coefficient of the link from antenna k at BS S to antenna n at user U_m .

For TAS/MRC, \hat{k} , \hat{i} , and \hat{j} are given by [30]

$$\left(\hat{k}, \hat{i}\right) = \arg \max_{1 \leq k \leq N_S, 1 \leq i \leq I} \left\{ \left\| \mathbf{h}_{S_k H_i} \right\|^2 \right\}, \quad (3)$$

and

$$\hat{j} = \arg \max_{1 \leq j \leq J} \left\{ \left\| \mathbf{h}_{S_k L_j} \right\|^2 \right\}, \quad (4)$$

where $\mathbf{h}_{S_k U_m}$ represents the $N_U \times 1$ channel vector of $S_k \rightarrow U_m$ link.

2) *LCS Method*: To improve the performance of the selected user in cluster L which has a lower priority, an antenna at BS S and a user in cluster L are jointly chosen for transmission to provide the best channel power gain of the link from BS S to the selected user. Mathematically, \hat{k} , \hat{i} , \hat{j} , \hat{r}_H , and \hat{r}_L in this method can be expressed as follows:

For TAS/SC:

$$\begin{cases} \left(\hat{k}, \hat{j}, \hat{r}_L\right) = \arg \max_{1 \leq k \leq K_S, 1 \leq j \leq J, 1 \leq r \leq K_L} \left\{ \left| h_{S_k L_{j,r}} \right|^2 \right\}, \\ \left(\hat{i}, \hat{r}_H\right) = \arg \max_{1 \leq i \leq I, 1 \leq r \leq K_H} \left\{ \left| h_{S_k H_{i,r}} \right|^2 \right\}, \end{cases} \quad (5)$$

and for TAS/MRC:

$$\begin{cases} \left(\hat{k}, \hat{j}\right) = \arg \max_{1 \leq k \leq N_S, 1 \leq j \leq J} \left\{ \left\| \mathbf{h}_{S_k L_j} \right\|^2 \right\}, \\ \hat{i} = \arg \max_{1 \leq i \leq I} \left\{ \left\| \mathbf{h}_{S_k H_i} \right\|^2 \right\}, \end{cases} \quad (6)$$

B. Information Transmission Process and Channel Statistics

With the NOMA protocol, BS S transmits the mixed message [35]

$$x = \sqrt{P_S \alpha_{H_i}} x_{H_i} + \sqrt{P_S \alpha_{L_j}} x_{L_j} \quad (7)$$

to H_i and L_j . Herein, P_S is the total transmit power, α_{H_i} and α_{L_j} ($\alpha_{H_i} + \alpha_{L_j} = 1$) denote the power allocation coefficients, as well as x_{H_i} and x_{L_j} represent the messages for users H_i and L_j , respectively. It is noted that $\alpha_{H_i} > \alpha_{L_j} > 0$ due to higher priority of user H_i . Thus, the received signal at user U ($U \in \{H_i, L_j\}$) is given by

$$y_U = \mathbf{u}_U \mathbf{h}_{S_k U} \sqrt{P_S} \left(\sqrt{\alpha_{H_i}} x_{H_i} + \sqrt{\alpha_{L_j}} x_{L_j} \right) + \mathbf{u}_U \mathbf{w}_U, \quad (8)$$

where $\mathbf{w}_U \sim \mathcal{CN}(0, N_0)$ denotes the additive white Gaussian noise (AWGN) at user U , and \mathbf{u}_U represents the signal processing operation at user U , which is defined as in [38]

$$\mathbf{u}_U = \begin{cases} \mathbf{e}_{K_U, \hat{r}_U}, & \text{for TAS/SC} \\ \frac{\mathbf{h}_{S_k U}^\dagger}{\left\| \mathbf{h}_{S_k U} \right\|}, & \text{for TAS/MRC} \end{cases}, \quad (9)$$

where $\mathbf{e}_{K,i}$ is a $1 \times K$ vector whose the i -th element is equal to 1, and the others are zeros.

According to NOMA principle, the user H_i can directly decode its own message, x_{H_i} , since it is allocated with larger transmit power (i.e., $\alpha_{H_i} > \alpha_{L_j}$), hence, the interference generated by the signal of the user L_j , x_{L_j} , can be treated

as noise [31]. Thus, the instantaneous signal-to-interference-plus-noise ratio (SINR) at user H_i to detect x_{H_i} is written as

$$\gamma_{H_i}^{x_{H_i}} = \frac{\alpha_{H_i} \gamma_0 g_{SH}}{\alpha_{L_j} \gamma_0 g_{SH} + 1}, \quad (10)$$

where $\gamma_0 = \frac{P_S}{N_0}$ denotes the average transmit SNR and g_{SH} is defined as

$$g_{SH} = \begin{cases} \left| h_{S_k H_i, \hat{r}_H} \right|^2, & \text{for TAS/SC} \\ \left\| \mathbf{h}_{S_k H_i} \right\|^2, & \text{for TAS/MRC} \end{cases} \quad (11)$$

Meanwhile, the user L_j utilizes SIC to first decode x_{H_i} and then remove this component from the received signal before detecting its own message, x_{L_j} , [31]. Thus, the instantaneous SINR and SNR at L_j to detect x_{H_i} and x_{L_j} are respectively expressed as

$$\gamma_{L_j}^{x_{H_i}} = \frac{\alpha_{H_i} \gamma_0 g_{SL}}{\alpha_{L_j} \gamma_0 g_{SL} + 1}, \quad (12)$$

and

$$\gamma_{L_j}^{x_{L_j}} = \alpha_{L_j} \gamma_0 g_{SL}, \quad (13)$$

where g_{SL} is given by

$$g_{SL} = \begin{cases} \left| h_{S_k L_j, \hat{r}_L} \right|^2, & \text{for TAS/SC} \\ \left\| \mathbf{h}_{S_k L_j} \right\|^2, & \text{for TAS/MRC} \end{cases} \quad (14)$$

III. PROPOSED APPROACH FOR BLER PERFORMANCE ANALYSIS WITH SPC

In this section, we present some preliminaries on SPC and average BLER calculation, the derivation of CDF of channel power gains, and the average BLER analysis by utilizing HCS and LCS methods with TAS/SC and TAS/MRC schemes, specified in Section II-A.

A. Preliminaries

Considering SPC with blocklength N_U ($U \in \{H_i, L_j\}$) and the number of information bits n_U to user U , the instantaneous BLER of decoding x_V ($V \in \{H_i, L_j\}$) at user U is approximated as in [24]

$$\varepsilon_U^{x_V} \approx Q \left(\frac{\log_2(1 + \gamma_U^{x_V}) - n_V/N_V}{\sqrt{v_U^{x_V}/N_V}} \right), \quad (15)$$

where $Q(x) = \int_x^\infty \frac{1}{\sqrt{2\pi}} e^{-t^2/2} dt$ denotes the Gaussian Q-function and $v_U^{x_V} = (\log_2 e)^2 \left[1 - \frac{1}{(1 + \gamma_U^{x_V})} \right]$ represents the channel dispersion. From (15), the average BLER $\bar{\varepsilon}_U^{x_V}$ has the following form

$$\bar{\varepsilon}_U^{x_V} \approx \int_0^\infty \varepsilon_U^{x_V} f_{\gamma_U^{x_V}}(x) dx, \quad (16)$$

where $f_X(x)$ is the probability density function (PDF) of a random variable X . It is challenging to derive $\bar{\varepsilon}_U^{x_V}$ in (16).

Therefore, an approximation of ε_U^{xV} is utilized as discussed in [39], i.e.,

$$\varepsilon_U^{xV} \approx \begin{cases} 1, & \gamma_U^{xV} \leq v_V \\ A_U^{xV}, & v_V < \gamma_U^{xV} < \mu_V \\ 0, & \gamma_U^{xV} \geq \mu_V \end{cases}, \quad (17)$$

where $A_U^{xV} = 0.5 - \chi_V \sqrt{N_V} (\gamma_U^{xV} - \beta_V)$, $\chi_V = \sqrt{\frac{1}{2\pi} \left(\frac{2^{2N_V}}{2^{2N_V} - 1} \right)}$, $v_V = \beta_V - \frac{1}{2\chi_V \sqrt{N_V}}$, $\mu_V = \beta_V + \frac{1}{2\chi_V \sqrt{N_V}}$, and $\beta_V = 2^{\frac{N_V}{2}} - 1$. By substituting (17) into (16), $\bar{\varepsilon}_U^{xV}$ can be rewritten as

$$\bar{\varepsilon}_U^{xV} \approx \chi_V \sqrt{N_V} \int_{v_V}^{\mu_V} F_{\gamma_U^{xV}}(x) dx. \quad (18)$$

For user $H_{\hat{i}}$, from (10) and (18), its average BLER is expressed as

$$\begin{aligned} \bar{\varepsilon}_{H_{\hat{i}}} &= \bar{\varepsilon}_{H_{\hat{i}}}^{xH_{\hat{i}}} \\ &\approx \chi_{H_{\hat{i}}} \sqrt{N_{H_{\hat{i}}}} \int_{v_{H_{\hat{i}}}}^{\mu_{H_{\hat{i}}}} F_{\gamma_{H_{\hat{i}}}}(x) dx. \end{aligned} \quad (19)$$

For user $L_{\hat{j}}$, it needs to decode the message of user $H_{\hat{i}}$, $x_{H_{\hat{i}}}$, before detecting its own message, $x_{L_{\hat{j}}}$. Therefore, the average BLER at user $L_{\hat{j}}$ is given by

$$\bar{\varepsilon}_{L_{\hat{j}}} = \bar{\varepsilon}_{L_{\hat{j}}}^{xH_{\hat{i}}} + \left(1 - \bar{\varepsilon}_{L_{\hat{j}}}^{xH_{\hat{i}}}\right) \bar{\varepsilon}_{L_{\hat{j}}}^{xL_{\hat{j}}}, \quad (20)$$

where

$$\bar{\varepsilon}_{L_{\hat{j}}}^{xH_{\hat{i}}} \approx \chi_{H_{\hat{i}}} \sqrt{N_{H_{\hat{i}}}} \int_{v_{H_{\hat{i}}}}^{\mu_{H_{\hat{i}}}} F_{\gamma_{L_{\hat{j}}}}(x) dx,$$

and

$$\bar{\varepsilon}_{L_{\hat{j}}}^{xL_{\hat{j}}} \approx \chi_{L_{\hat{j}}} \sqrt{N_{L_{\hat{j}}}} \int_{v_{L_{\hat{j}}}}^{\mu_{L_{\hat{j}}}} F_{\gamma_{L_{\hat{j}}}}(x) dx.$$

B. Derivation for Cumulative Distribution Function (CDF) of Channel Power Gains

To derive the average BLER at users $H_{\hat{i}}$ and $L_{\hat{j}}$, we first need to calculate the CDFs of g_{SH} and g_{SL} with TAS/SC and TAS/MRC schemes in both HCS and LCS methods. This is described as follows:

1) *HCS Method*: The CDFs of g_{SH} and g_{SL} with HCS method are derived in the following propositions.

Proposition 1. *Under HCS method and Nakagami- m fading, the CDF of g_{SH} with TAS/SC and TAS/MRC schemes is given by*

$$F_{g_{SH}}^{HCS}(x) = 1 + \sum_{p=1}^{a_{H,I}} \sum_{\Delta_H=p} \Phi_H c_{H,I} x^{\varphi_H} e^{-\frac{p m_H x}{\lambda_{SH}}}, \quad (21)$$

where $\Delta_H = \sum_{q=0}^{b_H-1} \delta_{H,q}$, $\varphi_H = \sum_{q=0}^{b_H-1} q \delta_{H,q}$, $\Phi_H = (-1)^p \left[\prod_{q=0}^{b_H-1} \left(\frac{m_H^q}{q! \lambda_{SH}^q} \right)^{\delta_{H,q}} \right]$, $\lambda_{SH} =$

$d_{SH}^{-\theta}$, $a_{H,I} = \begin{cases} K_S K_H I, & \text{for TAS/SC} \\ K_S I, & \text{for TAS/MRC} \end{cases}$, $b_H = \begin{cases} m_H, & \text{for TAS/SC} \\ m_H K_H, & \text{for TAS/MRC} \end{cases}$, and $c_{H,I} = \binom{a_{H,I}}{p} \binom{p}{\delta_{H,0}, \dots, \delta_{H,b_H-1}}$, d_{SH} and θ denote the distance and path loss exponent of the link from BS S to user $H_{\hat{i}}$, respectively.

Proof: See Appendix A. \blacksquare

Proposition 2. *Under HCS method and Nakagami- m fading, the CDF of g_{SL} with TAS/SC and TAS/MRC schemes is expressed as*

$$F_{g_{SL}}^{HCS}(x) = 1 + \sum_{p=1}^{a_{L,I}} \sum_{\Delta_L=p} \Phi_L c_{L,I} x^{\varphi_L} e^{-\frac{p m_L x}{\lambda_{SL}}}, \quad (22)$$

where $\Delta_L = \sum_{q=0}^{b_L-1} \delta_{L,q}$, $\varphi_L = \sum_{q=0}^{b_L-1} q \delta_{L,q}$, $\Phi_L = (-1)^p \left[\prod_{q=0}^{b_L-1} \left(\frac{m_L^q}{q! \lambda_{SL}^q} \right)^{\delta_{L,q}} \right]$, $\lambda_{SL} = d_{SL}^{-\theta}$, $a_{L,I} = \begin{cases} K_L J, & \text{for TAS/SC} \\ J, & \text{for TAS/MRC} \end{cases}$, $b_L = \begin{cases} m_L, & \text{for TAS/SC} \\ m_L K_L, & \text{for TAS/MRC} \end{cases}$, and $c_{L,I} = \binom{a_{L,I}}{p} \binom{p}{\delta_{L,0}, \dots, \delta_{L,b_L-1}}$, d_{SL} and θ denotes the distance of the link from BS S to user $L_{\hat{j}}$, respectively.

Proof: It is noted that TAS is used to select the best transmit antenna for user $H_{\hat{i}}$ in this case, hence, it is considered as a random solution for user $L_{\hat{j}}$. As such, using (1), (2), (3), and (4), the CDF of g_{SL} is given by [30, 40]

$$F_{g_{SL}}(x) = \left(1 - \sum_{p=0}^{b_L-1} \frac{m_L^p}{p! \lambda_{SL}^p} x^p e^{-\frac{m_L x}{\lambda_{SL}}} \right)^{a_{L,I}}. \quad (23)$$

By using binomial expansion and multinomial theorem similar to the proof of Proposition 1 in Appendix A, we obtain the final expression of $F_{g_{SL}}(x)$ as in (22) and the proof is completed. \blacksquare

2) *LCS Method*: Utilizing (5), (6), and algebraic manipulations similar to the proof of Proposition 1 in Appendix A, the CDF of g_{SH} and g_{SL} in this case are expressed as

$$F_{g_{SH}}^{LCS}(x) = 1 + \sum_{p=1}^{a_{H,II}} \sum_{\Delta_H=p} \Phi_H c_{H,II} x^{\varphi_H} e^{-\frac{p m_H x}{\lambda_{SH}}}, \quad (24)$$

and

$$F_{g_{SL}}^{LCS}(x) = 1 + \sum_{p=1}^{a_{L,II}} \sum_{\Delta_L=p} \Phi_L c_{L,II} x^{\varphi_L} e^{-\frac{p m_L x}{\lambda_{SL}}}, \quad (25)$$

where $a_{H,II} = \begin{cases} K_H I, & \text{for TAS/SC} \\ I, & \text{for TAS/MRC} \end{cases}$, $c_{H,II} = \binom{a_{H,II}}{p} \binom{p}{\delta_{H,0}, \dots, \delta_{H,b_H-1}}$, $a_{L,II} = \begin{cases} K_S K_L J, & \text{for TAS/SC} \\ K_S J, & \text{for TAS/MRC} \end{cases}$, and $c_{L,II} = \binom{a_{L,II}}{p} \binom{p}{\delta_{L,0}, \dots, \delta_{L,b_L-1}}$.

C. Average BLER Analysis of HCS Method

The derivation of the average BLER at users H_i and L_j in case of using the TAS/SC or TAS/MRC scheme with HCS method are provided in the following theorems.

Theorem 1. Under HCS method and Nakagami- m fading, the average BLER at user H_i utilizing TAS/SC or TAS/MRC is expressed as

$$\begin{aligned} \bar{\varepsilon}_{H_i}^{HCS} &\approx 1 + \frac{\chi_{H_i} \alpha_{H_i} \sqrt{N_{H_i}}}{\gamma_0 \alpha_{L_j}^2} \sum_{p=1}^{a_{H,i}} \sum_{\Delta_H=p}^{\varphi_H} \sum_{q=0}^{\varphi_H} \binom{\varphi_H}{q} \\ &\times \left(-\frac{1}{\gamma_0 \alpha_{L_j}} \right)^q \Phi_{HCH,II} e^{\frac{\omega_H}{\gamma_0 \alpha_{L_j}}} \mathcal{A}_H, \end{aligned} \quad (26)$$

where

$$\mathcal{A}_H = \begin{cases} \omega_H \Xi_{H,1} + \Xi_{H,2}, & \hat{\varphi}_H = -2 \\ -\Xi_{H,1}, & \hat{\varphi}_H = -1 \\ \omega_H^{-\hat{\varphi}_H - 1} \Xi_{H,3}, & \hat{\varphi}_H \geq 0 \end{cases},$$

$$\begin{aligned} \omega_H &= \frac{pm_H}{\lambda_{SH} H_i}, \quad \Xi_{H,1} = \text{Ei}(-\omega_H \phi_{H_i}) - \text{Ei}(-\omega_H \kappa_{H_i}), \\ \Xi_{H,2} &= \frac{e^{-\omega_H \phi_{H_i}}}{\phi_{H_i}} - \frac{e^{-\omega_H \kappa_{H_i}}}{\kappa_{H_i}}, \quad \Xi_{H,3} = \Gamma(\hat{\varphi}_H + 1, \omega_H \phi_{H_i}) - \\ &\Gamma(\hat{\varphi}_H + 1, \omega_H \kappa_{H_i}), \quad \phi_{H_i} = \frac{1}{\gamma_0 \alpha_{L_j}} + B_{v_{H_i}}, \quad \kappa_{H_i} = \frac{1}{\gamma_0 \alpha_{L_j}} + \\ &B_{\mu_{H_i}}, \quad B_x = \frac{x}{\gamma_0 (\alpha_{H_i} - \alpha_{L_j} x)}, \quad \text{and } \hat{\varphi}_H = \varphi_H - q - 2. \end{aligned}$$

Proof: See Appendix B. ■

Theorem 2. Under HCS method and Nakagami- m fading, the average BLER at user L_j utilizing TAS/SC or TAS/MRC is given by

$$\bar{\varepsilon}_{L_j}^{HCS} = \bar{\varepsilon}_{L_j}^{x_{H_i}, HCS} + \left(1 - \bar{\varepsilon}_{L_j}^{x_{H_i}, HCS} \right) \bar{\varepsilon}_{L_j}^{x_{L_j}, HCS}, \quad (27)$$

where

$$\begin{aligned} \bar{\varepsilon}_{L_j}^{x_{H_i}, HCS} &\approx 1 + \frac{\chi_{H_i} \alpha_{H_i} \sqrt{N_{H_i}}}{\gamma_0 \alpha_{L_j}^2} \sum_{p=1}^{a_{L,i}} \sum_{\Delta_L=p}^{\varphi_L} \sum_{q=0}^{\varphi_L} \binom{\varphi_L}{q} \\ &\times \left(-\frac{1}{\gamma_0 \alpha_{L_j}} \right)^q \Phi_{LCL,IE} e^{\frac{\omega_L}{\gamma_0 \alpha_{L_j}}} \mathcal{A}_L, \end{aligned}$$

$$\bar{\varepsilon}_{L_j}^{x_{L_j}, HCS} \approx 1 + \chi_{L_j} \sqrt{N_{L_j}} \sum_{p=1}^{a_{L,i}} \sum_{\Delta_L=p}^{\varphi_L} \frac{\Phi_{LCL,II} \hat{\omega}_L^{-\varphi_L - 1}}{(\alpha_{L_j} \gamma_0)^{\varphi_L}} \Xi_{L,4},$$

$$\mathcal{A}_L = \begin{cases} \omega_L \Xi_{L,1} + \Xi_{L,2}, & \hat{\varphi}_L = -2 \\ -\Xi_{L,1}, & \hat{\varphi}_L = -1 \\ \omega_L^{-\hat{\varphi}_L - 1} \Xi_{L,3}, & \hat{\varphi}_L \geq 0 \end{cases},$$

$$\begin{aligned} \Xi_{L,1} &= \text{Ei}(-\omega_L \phi_{H_i}) - \text{Ei}(-\omega_L \kappa_{H_i}), \quad \Xi_{L,2} = \frac{e^{-\omega_L \phi_{H_i}}}{\phi_{H_i}} - \\ &\frac{e^{-\omega_L \kappa_{H_i}}}{\kappa_{H_i}}, \quad \Xi_{L,3} = \Gamma(\hat{\varphi}_L + 1, \omega_L \phi_{H_i}) - \Gamma(\hat{\varphi}_L + 1, \omega_L \kappa_{H_i}), \\ \Xi_{L,4} &= \Gamma(\varphi_L + 1, \hat{\omega}_L v_{L_j}) - \Gamma(\varphi_L + 1, \hat{\omega}_L \mu_{L_j}), \quad \omega_L = \\ &\frac{pm_L}{\lambda_{SL}}, \quad \hat{\varphi}_L = \varphi_L - q - 2, \quad \text{and } \hat{\omega}_L = \frac{pm_L}{\lambda_{SL} \alpha_{L_j} \gamma_0}. \end{aligned}$$

Proof: See Appendix C. ■

D. Average BLER Analysis of LCS Method

In this case, the average BLER at user H_i and L_j are derived through the following theorems.

Theorem 3. Under LCS method and Nakagami- m fading, the average BLER at user H_i with TAS/SC or TAS/MRC is expressed as

$$\begin{aligned} \bar{\varepsilon}_{H_i}^{LCS} &\approx 1 + \frac{\chi_{H_i} \alpha_{H_i} \sqrt{N_{H_i}}}{\gamma_0 \alpha_{L_j}^2} \sum_{p=1}^{a_{H,II}} \sum_{\Delta_H=p}^{\varphi_H} \sum_{q=0}^{\varphi_H} \binom{\varphi_H}{q} \\ &\times \left(-\frac{1}{\gamma_0 \alpha_{L_j}} \right)^q \Phi_{HCH,II} e^{\frac{\omega_H}{\gamma_0 \alpha_{L_j}}} \mathcal{A}_H. \end{aligned} \quad (28)$$

Proof: To derive $\bar{\varepsilon}_{H_i}^{LCS}$ in this theorem, the algebraic manipulations similar to the derivation of $\bar{\varepsilon}_{H_i}^{HCS}$ in Appendix B can be utilized, where (24) is employed instead of (21). ■

Theorem 4. Under LCS method and Nakagami- m fading, the average BLER at user L_j with TAS/SC or TAS/MRC is given by

$$\bar{\varepsilon}_{L_j}^{LCS} = \bar{\varepsilon}_{L_j}^{x_{H_i}, LCS} + \left(1 - \bar{\varepsilon}_{L_j}^{x_{H_i}, LCS} \right) \bar{\varepsilon}_{L_j}^{x_{L_j}, LCS}, \quad (29)$$

where

$$\begin{aligned} \bar{\varepsilon}_{L_j}^{x_{H_i}, LCS} &\approx 1 + \frac{\chi_{H_i} \alpha_{H_i} \sqrt{N_{H_i}}}{\gamma_0 \alpha_{L_j}^2} \sum_{p=1}^{a_{L,II}} \sum_{\Delta_L=p}^{\varphi_L} \sum_{q=0}^{\varphi_L} \binom{\varphi_L}{q} \\ &\times \left(-\frac{1}{\gamma_0 \alpha_{L_j}} \right)^q \Phi_{LCL,IE} e^{\frac{\omega_L}{\gamma_0 \alpha_{L_j}}} \mathcal{A}_L, \end{aligned}$$

and

$$\bar{\varepsilon}_{L_j}^{x_{L_j}, LCS} \approx 1 + \chi_{L_j} \sqrt{N_{L_j}} \sum_{p=1}^{a_{L,II}} \sum_{\Delta_L=p}^{\varphi_L} \frac{\Phi_{LCL,II} \hat{\omega}_L^{-\varphi_L - 1}}{(\alpha_{L_j} \gamma_0)^{\varphi_L}} \Xi_{L,4}.$$

Proof: The proof of this theorem can be carried out in the same way as the proof of Theorem 2, where (25) is used instead of (22). ■

IV. PROPOSED ANALYTICAL FRAMEWORK FOR OPTIMAL POWER ALLOCATION AND MINIMUM BLOCKLENGTH

By following the average BLER analysis presented in Section III, this section provides the derivation of the optimal power allocation coefficients for a minimum blocklength based on asymptotic average BLER in high SNR regime, and it also presents the analytical comparison of the minimum blocklength of NOMA with the OMA case.

A. Asymptotic Average BLER Analysis

As discussed in [24, 25], the average BLER, $\bar{\varepsilon}_U^{xV}$, in (18) can be simplified by utilizing the first-order Riemann integral approximation, i.e., $\int_a^b f(x) dx = (b-a)f\left(\frac{a+b}{2}\right)$, as follows:

$$\bar{\varepsilon}_U^{xV} \approx \chi_V \sqrt{N_V} (\mu_V - v_V) F_{\gamma_U^{xV}} \left(\frac{v_V + \mu_V}{2} \right). \quad (30)$$

By substituting v_V and μ_V defined in (16) into (30), $\bar{\varepsilon}_U^{xV}$ is rewritten as

$$\bar{\varepsilon}_U^{xV} \approx F_{\gamma_U^{xV}}(\beta_V), \quad (31)$$

where β_V is defined in (17).

By using the series representation of e^x in [41, Eq. 1.211], i.e., $e^x = \sum_{k=0}^{\infty} \frac{x^k}{k!}$, the asymptotic CDF of $\gamma_{H_i}^{x_{H_i}}$, $\gamma_{L_j}^{x_{L_j}}$, and $\gamma_{L_j}^{x_{L_j}}$ are respectively given by

$$F_{\gamma_{H_i}}^{s,\infty}(x) = F_{g_{SH}}^{s,\infty}(B_x) \stackrel{\gamma_0 \rightarrow \infty}{\approx} \frac{(m_H B_x)^{b_H a_{H,r}}}{(b_H!)^{a_{H,r}} \lambda_{SH}^{b_H a_{H,r}}}, \quad (32)$$

$$F_{\gamma_{L_j}}^{s,\infty}(x) \stackrel{\gamma_0 \rightarrow \infty}{\approx} \frac{(m_L B_x)^{b_L a_{L,r}}}{(b_L!)^{a_{L,r}} \lambda_{SL}^{b_L a_{L,r}}}, \quad (33)$$

and

$$F_{\gamma_{L_j}}^{s,\infty}(x) \stackrel{\gamma_0 \rightarrow \infty}{\approx} \frac{(m_L \hat{B}_x)^{b_L a_{L,r}}}{(b_L!)^{a_{L,r}} \lambda_{SL}^{b_L a_{L,r}}}, \quad (34)$$

where $s \in \{HCS, LCS\}$, $r = \begin{cases} I, & \text{if } s = HCS \\ II, & \text{if } s = LCS \end{cases}$, $B_x = \frac{x}{\gamma_0(\alpha_{H_i} - \alpha_{L_j} x)}$, and $\hat{B}_x = \frac{x}{\alpha_{L_j} \gamma_0}$. From (30) - (34), the asymptotic average BLER at users H_i and L_j are respectively expressed as

$$\bar{\varepsilon}_{H_i}^{s,\infty} \approx \frac{(m_H B_{\beta_{H_i}})^{b_H a_{H,r}}}{(b_H!)^{a_{H,r}} \lambda_{SH}^{b_H a_{H,r}}}, \quad (35)$$

and

$$\begin{aligned} \bar{\varepsilon}_{L_j}^{s,\infty} &= \bar{\varepsilon}_{L_j,\infty}^{x_{H_i},s} + \left(1 - \bar{\varepsilon}_{L_j,\infty}^{x_{H_i},s}\right) \bar{\varepsilon}_{L_j,\infty}^{x_{L_j},s} \\ &\approx \bar{\varepsilon}_{L_j,\infty}^{x_{H_i},s} + \bar{\varepsilon}_{L_j,\infty}^{x_{L_j},s} \\ &\approx \frac{(m_L B_{\beta_{H_i}})^{b_L a_{L,r}}}{(b_L!)^{a_{L,r}} \lambda_{SL}^{b_L a_{L,r}}} + \frac{(m_L \hat{B}_{\beta_{L_j}})^{b_L a_{L,r}}}{(b_L!)^{a_{L,r}} \lambda_{SL}^{b_L a_{L,r}}}. \end{aligned} \quad (36)$$

From (35) and (36), the diversity order at users H_i and L_j are respectively given by [36]

$$\begin{aligned} D_{H_i} &= - \lim_{\gamma_0 \rightarrow \infty} \frac{\log(\bar{\varepsilon}_{H_i}^{s,\infty})}{\log(\gamma_0)} \\ &= \begin{cases} m_H K_S K_H I, & \text{for HCS method} \\ m_H K_H I, & \text{for LCS method} \end{cases}, \end{aligned} \quad (37)$$

and

$$\begin{aligned} D_{L_j} &= - \lim_{\gamma_0 \rightarrow \infty} \frac{\log(\bar{\varepsilon}_{L_j}^{s,\infty})}{\log(\gamma_0)} \\ &= \begin{cases} m_L K_L J, & \text{for HCS method} \\ m_L K_S K_L J, & \text{for LCS method} \end{cases}. \end{aligned} \quad (38)$$

Remark 1. For both TAS/SC and TAS/MRC schemes, the diversity orders at users H_i and L_j , denoted by (D_{H_i}, D_{L_j}) , are $(m_H K_S K_H I, m_L K_L J)$ for HCS method, and $(m_H K_H I, m_L K_S K_L J)$ for LCS method. This reveals that the users H_i and L_j have achieved full diversity order with HCS and LCS methods, respectively. Furthermore, the system performance of user H_i can be improved by increasing m_H , K_S , K_H , and I with HCS method, and by increasing m_H , K_H , and I with LCS method. Meanwhile, the growth of

m_L , K_L , and J with HCS method, and m_L , K_S , K_L , and J with LCS method can help enhancing the system performance of user L_j .

B. Power and Blocklength Optimization at High SNR

To determine the values of power allocation coefficients (i.e., α_{H_i} and α_{L_j}) at which a minimum blocklength N_U ($U \in \{H_i, L_j\}$) is achieved to guarantee the reliability target $\bar{\varepsilon}_U^{th}$, the following problem needs to be addressed

$$\min_{\alpha_{H_i}, \alpha_{L_j}} N_U \quad (39a)$$

$$\text{s.t.} \quad \bar{\varepsilon}_U \leq \bar{\varepsilon}_U^{th}, \quad (39b)$$

$$\alpha_{H_i} + \alpha_{L_j} = 1, \quad 0 < \alpha_{L_j} < 0.5. \quad (39c)$$

It is noted that $\alpha_{H_i} = 1 - \alpha_{L_j}$ and $\bar{\varepsilon}_U$ is a decreasing function of N_U . The problem in (39) can be simplified as

$$\min_{\alpha_{L_j}} N_U \quad (40a)$$

$$\text{s.t.} \quad \bar{\varepsilon}_U = \bar{\varepsilon}_U^{th}, \quad (40b)$$

$$0 < \alpha_{L_j} < 0.5. \quad (40c)$$

By substituting (35) into (40b) for user H_i and (36) into (40b) for user L_j , the blocklengths of users H_i and L_j with s ($s \in \{HCS, LCS\}$) method are respectively calculated as

$$N_{H_i,s} = \frac{n_{H_i}}{\log_2 \left(\frac{1 + \left(\bar{\varepsilon}_{H_i,r}^{th} / \eta_{H,r} \right)^{1/b_H a_{H,r}}}{1 + \alpha_{L_j} \left(\bar{\varepsilon}_{H_i,r}^{th} / \eta_{H,r} \right)^{1/b_H a_{H,r}}} \right)}, \quad (41)$$

and

$$\begin{aligned} N_{L_j,s} &= \frac{n_{L_j}}{\log_2 \left(1 + \alpha_{L_j} \gamma_0 \left(\frac{\bar{\varepsilon}_{L_j,r}^{th} - \eta_{L,r} \left(\bar{\varepsilon}_{H_i,r}^{th} \right)^{\frac{b_L a_{L,r}}{b_H a_{H,r}}}}{\hat{\eta}_{L,r}} \right)^{1/b_L a_{L,r}} \right)}, \end{aligned} \quad (42)$$

where $\eta_{H,r} = \frac{m_H^{b_H a_{H,r}}}{(b_H!)^{a_{H,r}} \lambda_{SH}^{b_H a_{H,r}} \gamma_0^{b_H a_{H,r}}}$, $\eta_{L,r} = \frac{(b_H!)^{\frac{b_L a_{L,r}}{b_H a_{H,r}}}}{(b_L!)^{a_{L,r}} \lambda_{SL}^{b_L a_{L,r}}} \left(\frac{m_L \lambda_{SH}}{m_H \lambda_{SL}} \right)^{b_L a_{L,r}}$, and $\hat{\eta}_{L,r} = \frac{m_L^{b_L a_{L,r}}}{(b_L!)^{a_{L,r}} \lambda_{SL}^{b_L a_{L,r}}}$.

From (41) and (42), the derivative of $N_{H_i,s}$ and $N_{L_j,s}$ with respect to α_{L_j} are derived as

$$\frac{\partial N_{H_i,s}}{\partial \alpha_{L_j}} = \frac{n_{H_i} \tau_{H,r}}{\left(1 + \alpha_{L_j} \tau_{H,r}\right) \left[\log_2 \left(\frac{1 + \tau_{H,r}}{1 + \alpha_{L_j} \tau_{H,r}} \right) \right]^2 \ln 2} > 0, \quad (43)$$

and

$$\frac{\partial N_{L_j,s}}{\partial \alpha_{L_j}} = - \frac{n_{L_j} \tau_{L,r}}{\left(1 + \alpha_{L_j} \tau_{L,r}\right) \left[\log_2 \left(1 + \alpha_{L_j} \tau_{L,r} \right) \right]^2 \ln 2} < 0, \quad (44)$$

Algorithm 1: Proposed Power Allocation Algorithm for SPC-Based MIMO NOMA System

Data : $n_{H_i}, n_{L_j}, \gamma_0, \bar{\varepsilon}_{H_i,r}^{th}, \bar{\varepsilon}_{L_j,r}^{th}, K_S, K_H, K_L, I, J, \lambda_{SH}, \lambda_{SL}$, and tolerance μ .
Result: Determine optimal power allocation coefficient $\alpha_{L_j,opt}$.

```

1 Initialize:  $\alpha_{L_j}^- \leftarrow 0, \alpha_{L_j}^+ \leftarrow 0.5$ , and  $\hat{\alpha}_{L_j} \leftarrow \frac{\alpha_{L_j}^- + \alpha_{L_j}^+}{2}$ ;
2 while  $|f(\hat{\alpha}_{L_j})| > \mu$  do
3   if  $f(\hat{\alpha}_{L_j}) f(\alpha_{L_j}^-) > 0$  then
4     | Set  $\alpha_{L_j}^- \leftarrow \hat{\alpha}_{L_j}$ ;
5   else
6     | Set  $\alpha_{L_j}^+ \leftarrow \hat{\alpha}_{L_j}$ ;
7   end
8   Set  $\hat{\alpha}_{L_j} \leftarrow \frac{\alpha_{L_j}^- + \alpha_{L_j}^+}{2}$  and compute  $f(\hat{\alpha}_{L_j})$  based
   on (41) and (42);
9 end
10 Set  $\alpha_{L_j,opt} \leftarrow \hat{\alpha}_{L_j}$ ;
11 Return  $\alpha_{L_j,opt}$ ;

```

where $\tau_{H,r} = \left(\frac{\bar{\varepsilon}_{H_i,r}^{th}}{\eta_{H,r}}\right)^{1/b_H a_{H,r}}$ and $\tau_{L,r} = \gamma_0 \left[\frac{\bar{\varepsilon}_{L_j,r}^{th} - \eta_{L,r} \left(\frac{\bar{\varepsilon}_{H_i,r}^{th}}{\eta_{L,r}}\right)^{b_L a_{L,r}}}{\eta_{L,r}}\right]^{1/b_L a_{L,r}}$. Thus, $N_{H_i,s}$ is an increasing function of α_{L_j} , whereas $N_{L_j,s}$ is a decreasing function of α_{L_j} . Therefore, to guarantee both reliability targets $\bar{\varepsilon}_{H_i,r}^{th}$ and $\bar{\varepsilon}_{L_j,r}^{th}$, the minimum blocklength is obtained by addressing $N_{H_i,s} = N_{L_j,s} = N_{opt,s}$ and the problem of minimizing blocklength in (40) is rewritten as

$$\min_{\alpha_{L_j}} N_{opt,s} \quad (45a)$$

$$\text{s.t. } \bar{\varepsilon}_{H_i}^s = \bar{\varepsilon}_{H_i,r}^{th}, \quad (45b)$$

$$\bar{\varepsilon}_{L_j}^s = \bar{\varepsilon}_{L_j,r}^{th}, \quad (45c)$$

$$0 < \alpha_{L_j} < 0.5. \quad (45d)$$

Given this context, the optimal power allocation coefficient $\alpha_{L_j,opt}$ to minimize $N_{opt,s}$ can be achieved by solving the equation $f(\alpha_{L_j}) = N_{L_j,s} - N_{H_i,s} = 0$, which is addressed in Algorithm 1. The minimum blocklength $N_{opt,r}$ is attained by substituting $\alpha_{L_j,opt}$ into (41) as follows:

$$N_{opt,s} = \frac{n_{H_i}}{\log_2 \left(\frac{1 + \left(\frac{\bar{\varepsilon}_{H_i,r}^{th}}{\eta_{H,r}}\right)^{1/b_H a_{H,r}}}{1 + \alpha_{L_j,opt} \left(\frac{\bar{\varepsilon}_{H_i,r}^{th}}{\eta_{H,r}}\right)^{1/b_H a_{H,r}}} \right)}. \quad (46)$$

C. Comparison to OMA

With OMA transmission, the minimum blocklength, $N_{OMA,s}$ ($r \in \{I, II\}$), is the summation of the minimum blocklengths for users H_i and L_j , \hat{N}_{H_i} and \hat{N}_{L_j} . Similar to

the derivation of blocklengths for users H_i and L_j in Section IV-B, $N_{OMA,s}$ in the high SNR regime is calculated as

$$\begin{aligned} N_{OMA,s} &= \hat{N}_{H_i} + \hat{N}_{L_j} \\ &= \frac{n_{H_i}}{\log_2 \left[1 + \left(\frac{\bar{\varepsilon}_{H_i,r}^{th}}{\eta_{H,r}}\right)^{1/b_H a_{H,r}} \right]} \\ &\quad + \frac{n_{L_j}}{\log_2 \left[1 + \gamma_0 \left(\frac{\bar{\varepsilon}_{L_j,r}^{th}}{\eta_{L,r}}\right)^{1/b_L a_{L,r}} \right]}. \end{aligned} \quad (47)$$

From (46) and (47), the blocklength gap between NOMA and OMA, ΔN_s , is given by

$$\Delta N_r = N_{OMA,r} - N_{opt,r} \approx \hat{N}_{H_i,r} > 0. \quad (48)$$

Thus, OMA transmission needs a longer blocklength than NOMA transmission to serve the users H_i and L_j .

V. NUMERICAL RESULTS

In this section, we provide numerical results in terms of average BLER and minimum blocklength to characterize the effects of the proposed protocols, i.e., HCS and LCS methods with TAS/SC and TAS/MRC schemes discussed in Section II-A, on the system performance in designing an SPC-based MIMO NOMA network. It is noted that the analysis of these performance metrics have practical significance for the reliability and latency performance evaluation of wireless systems [24–29]. The predetermined simulation parameters are set as follows [24–26]: the number of information bits $n_{H_i} = n_{L_j} = 80$ bits; the blocklength $N_{H_i} = N_{L_j} = 100$; the path loss exponent $\theta = 2.5$; the distances $d_{SH} = d_{SL} = 5$ (m); the power allocation coefficients $\alpha_{H_i} = 0.7$, and $\alpha_{H_i} = 0.3$; the reliability targets $\bar{\varepsilon}_{H_i}^{th} = 10^{-7}$ and $\bar{\varepsilon}_{L_j}^{th} = 10^{-6}$.

In Figs. 2 and 3, we plot the average BLERs at users H_i and L_j as a function of γ_0 with different methods (i.e., HCS method with TAS/SC or TAS/MRC and LCS method with TAS/SC or TAS/MRC). As can be observed from these figures, the analytical results are almost in good agreement with the simulation results, and the asymptotic curves accurately predict the system performance trend in the higher γ_0 regime. This verifies the correctness of our analysis in Section III. In addition, Figs. 2 and 3 show that HCS method achieves better performance (i.e., lower value of average BLER is observed) for user H_i over LCS method, whereas LCS method outperforms HCS method in terms of the system performance for user L_j . This result is achieved based on the fact that HCS and LCS methods are proposed to improve the received signal quality at users H_i and L_j , respectively, as discussed in Section II-A. Furthermore, these figures indicate that TAS/MRC scheme is better than TAS/SC in improving the system performance.

In Figs. 4 and 5, we investigate the effects of the number of users at clusters H (I) and L (J), and the number of antennas at BS S (K_S), users H_i (K_H), and L_j (K_L), on the system performance. Specifically, Fig. 4 shows the variation of average BLER at user H_i with respect to γ_0 with different values of K_S, K_H , and I , denoted by (K_S, K_H, I) , in case of utilizing HCS and LCS methods with the TAS/SC scheme.

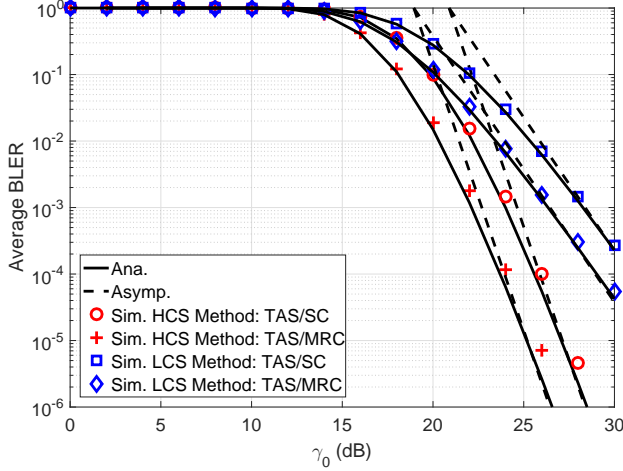


Fig. 2. Average BLER at user H_i vs. γ_0 with different methods, where $m_H = m_L = 2$ and $(K_S, K_H, I) = (2, 2, 1)$.

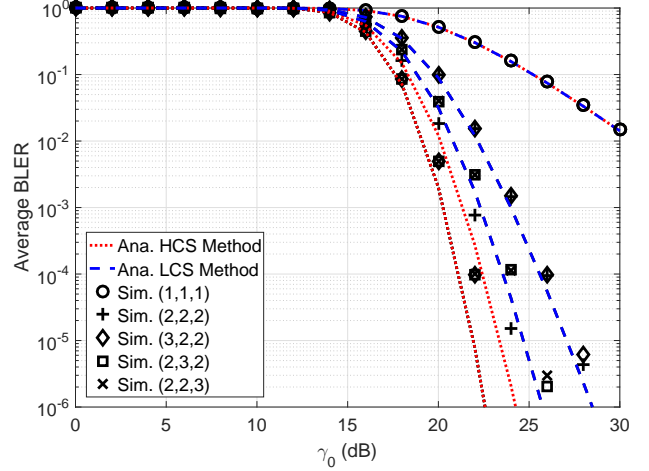


Fig. 4. Average BLER at user H_i vs. γ_0 with different values of (K_S, K_H, I) , where $m_H = m_L = 2$.

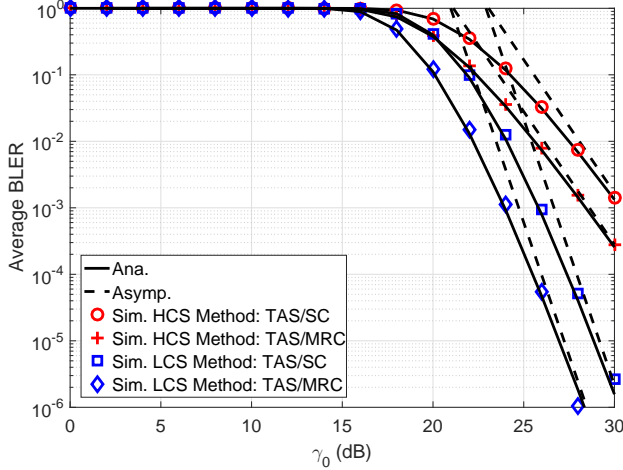


Fig. 3. Average BLER at user L_j vs. γ_0 with different methods, where $m_H = m_L = 2$ and $(K_S, K_L, J) = (2, 2, 1)$.

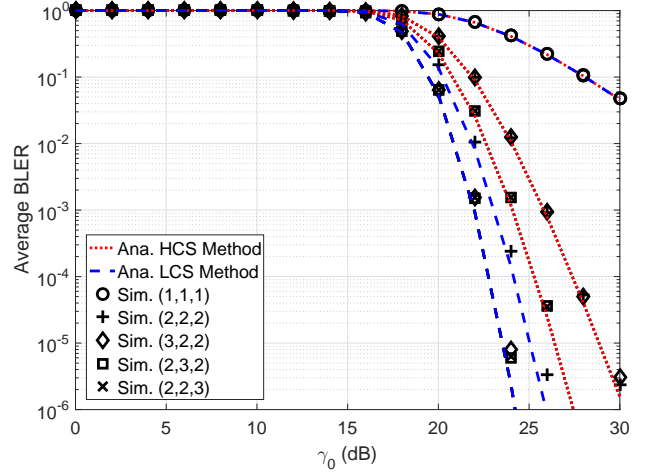


Fig. 5. Average BLER at user L_j vs. γ_0 with different values of (K_S, K_L, J) , where $m_H = m_L = 2$.

Meanwhile, Fig. 5 plots the average BLER at user L_j versus γ_0 with different values of (K_S, K_L, J) when using HCS and LCS methods with the TAS/SC scheme. These two figures indicate that as K_S, K_H, K_L, I , and J are all equal to one, HCS and LCS methods result in the same curves. Furthermore, the system performance can be significantly improved by increasing (K_S, K_H, I) for user H_i and (K_S, K_L, J) for user L_j . It is noted that the variation of K_S in LCS method does not impact the system performance at user H_i (see Fig. 4). The same conclusion can be derived for user L_j when observing the change of K_S in HCS method (see Fig. 5). The reason for this is based on the nature of HCS and LCS methods as mentioned in Section II-A and the discussion part of Figs. 2 and 3. This phenomenon also confirms our analysis of diversity order for users H_i and L_j , as shown in Section IV-A.

In Fig. 6, we consider the change of average BLER at users H_i and L_j with respect to the fading parameters, i.e., m_H and m_L , in case of using HCS and LCS methods with the

TAS/SC scheme. Herein, we set $m_H = m_L = m$. We can see from this figure that the system performance can be improved with the increase in m due to the better channel quality. More precisely, when $m = 1$, Nakagami- m fading corresponds to Rayleigh fading and the worst performance can be observed. In case of $m = (K+1)^2/(2K+1)$, it approximates the Rician fading with parameter K .

Fig. 7 depicts the effect of power allocation coefficient α_{L_j} on the blocklength of users H_i (N_{H_i}) and L_j (N_{L_j}). One can see from this figure that N_{H_i} and N_{L_j} are increasing and decreasing functions of α_{L_j} , respectively. Thus, there exists an optimal value of α_{L_j} , at which the minimum blocklength for both users H_i and L_j is achieved. The value of optimal α_{L_j} for different cases (i.e., HCS method with TAS/SC or TAS/MRC; LCS method with TAS/SC or TAS/MRC) can be found out by using Algorithm 1 and then the minimum blocklength is calculated by using (46).

In Fig. 8, we perform the minimum blocklength com-

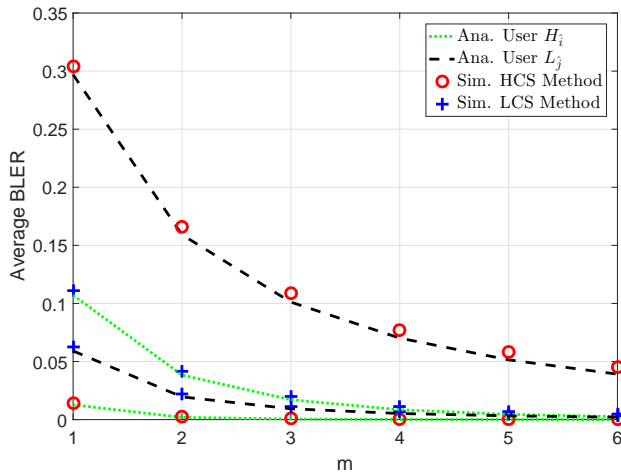


Fig. 6. Average BLER at users H_i and L_j vs. m with different methods, where $\gamma_0 = 20$ (dB) and $(K_S, K_H, K_L, I, J) = (2, 2, 2, 1, 1)$.

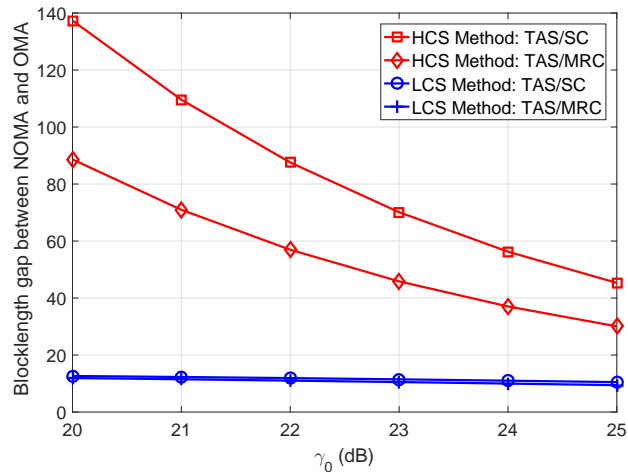


Fig. 8. Blocklength comparison between NOMA and OMA.

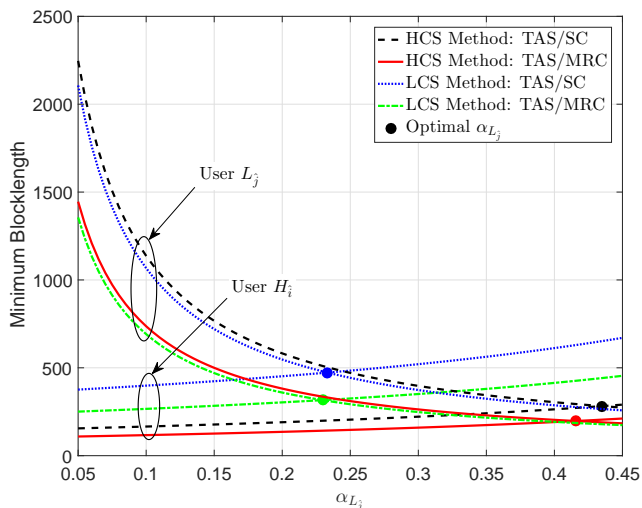


Fig. 7. Minimum blocklength for users H_i and L_j vs. α_{L_j} with different methods, where $m_h = m_L = 2$, $K_S = K_H = K_L = I = J = 2$, and $\gamma_0 = 20$ (dB).

parison between NOMA and OMA transmissions (N_{opt} and N_{OMA}) to clarify the benefits of NOMA over OMA in short-packet transmissions. As can be seen from this figure, the higher blocklength gap between NOMA and OMA, i.e., Δ_N (calculated from (48)), is achieved in case of using HCS method and TAS/SC scheme. This implies that the benefits of MIMO NOMA versus MIMO OMA in terms of minimum blocklength are more pronounced when utilizing HCS method as compared to LCS method. Furthermore, Δ_N is positive, hence, N_{opt} is always smaller than N_{OMA} . In other words, MIMO NOMA can lower the transmission latency of SPC systems as compared to the MIMO OMA case.

VI. CONCLUSIONS

In this paper, we analyzed the performance of short-packet transmission in a QoS-based multiuser downlink MIMO

NOMA system over a Nakagami- m fading channel in terms of the average BLER and minimum blocklength. Specifically, we considered the user pairing to perform NOMA, where users are selected from two user clusters having different priority levels. Furthermore, we investigated different MIMO schemes including TAS for BS, SC and MRC for users, and proposed two antenna-user selection methods, i.e., HCS and LCS to design effective communication protocols for the SPC-based MIMO NOMA systems. We characterized the system performance by deriving the approximate and asymptotic (in the high SNR regime) closed-form expressions of the average BLER at the users. From the asymptotic average BLER, we carried out an analysis of diversity order, minimum blocklength, and optimal power allocation. The analytical results verified by simulation results indicated that among the proposed schemes, the HCS method with TAS/MRC and the LCS method with TAS/MRC provide the best performance with full diversity gains for the users selected from the high-priority and low-priority user clusters, respectively. Moreover, it has been demonstrated that MIMO can significantly improve the performance of NOMA systems with short-packets, and MIMO NOMA outperforms MIMO OMA in ensuring low-latency transmissions.

APPENDIX A

PROOF OF PROPOSITION 1

Using (1) and (3), the CDF of g_{SH} in this case is given by [30]

$$F_{g_{SH}}^{HCS}(x) = \left(1 - \sum_{p=0}^{b_H-1} \frac{m_H^p}{p! \lambda_{SH}^p} x^p e^{-\frac{m_H x}{\lambda_{SH}}} \right)^{a_{H,I}}. \quad (49)$$

Applying binomial expansion in [41, Eq. (1.111)], (49) can be rewritten as

$$F_{g_{SH}}^{HCS}(x) = 1 + \underbrace{\sum_{p=1}^{a_{H,I}} \phi \left(\sum_{q=0}^{b_H-1} \frac{m_H^q x^q}{q! \lambda_{SH}^q} \right)^p}_{\Psi}, \quad (50)$$

where $\phi = \binom{a_{H,I}}{p} (-1)^p e^{-\frac{p m_H x}{\lambda_{SH}}}$.

To derive (50), we first resolve Ψ in (50) by utilizing the multinomial theorem as follows:

$$\Psi = \sum_{\Delta_H=p} \psi \left[\prod_{q=0}^{b_H-1} \left(\frac{m_H^q}{q! \lambda_{SH}^q} \right)^{\delta_{H,q}} \right] x^{\varphi_H}, \quad (51)$$

where $\psi = \binom{p}{\delta_{H,0}, \dots, \delta_{H,b_H-1}}$.

The final expression of $F_{\gamma_{SH}}^{HCS}(x)$ is achieved as in (21) by substituting (51) into (50).

APPENDIX B

PROOF OF THEOREM 1

From (10), the CDF of $\gamma_{H_i}^{x_{H_i}}$ is given by

$$F_{\gamma_{H_i}^{x_{H_i}}}(x) = \Pr \left\{ \frac{\alpha_{H_i} \gamma_0 g_{SH}}{\alpha_{L_j} \gamma_0 g_{SH} + 1} < x \right\} \quad (52)$$

$$= F_{g_{SH}}(B_x),$$

where (52) is obtained under the condition $\alpha_{H_i} - \alpha_{L_j} x > 0$ and $B_x = \frac{x}{\gamma_0(\alpha_{H_i} - \alpha_{L_j} x)}$ as defined in (26).

By substituting (52) into (19) and using (21), the average BLER at user H_i in HCS method with TAS/SC or TAS/MRC is expressed as

$$\bar{\varepsilon}_{H_i}^{HCS} \approx 1 + \chi_{H_i} \sqrt{N_{H_i}} \sum_{p=1}^{a_{H,i}} \sum_{\Delta_H=p} \Phi_{HCH,I}$$

$$\times \int_{v_{H_i}}^{\mu_{H_i}} B_x^{\varphi_H} e^{-\frac{p m_H B_x}{\lambda_{SH}}} dx, \quad (53)$$

To derive the integral in (53), we carry out the change of variable by letting $t = B_x$ and (53) can be rewritten as

$$\bar{\varepsilon}_{H_i}^{HCS} \approx 1 + \mathcal{A}_{H,1} \sum_{p=1}^{a_{H,i}} \sum_{\Delta_H=p} \Phi_{HCH,I} \int_{B_{v_{H_i}}}^{B_{\mu_{H_i}}} \frac{t^{\varphi_H} e^{-\frac{p m_H t}{\lambda_{SH}}}}{\left(\frac{1}{\gamma_0 \alpha_{L_j}} + t \right)^2} dt. \quad (54)$$

By letting $u = \frac{1}{\gamma_0 \alpha_{L_j}} + t$ and using binomial expansion [41, Eq. (1.111)], (54) has the following form

$$\bar{\varepsilon}_{H_i}^{HCS} \approx 1 + \mathcal{A}_{H,1} \underbrace{\sum_{H,i} \widetilde{c}_{H,I} \mathcal{A}_{H,2}}_{\mathcal{A}_{H,3}} \int_{\phi_{H_i}}^{\kappa_{H_i}} u^{\hat{\varphi}_H} e^{-\omega_H u} du. \quad (55)$$

We derive $\mathcal{A}_{H,3}$ in (55) with the aid of [41, Eqs. (3.351.4), (3.352.2), and (3.351.2)] and the final expression of $\bar{\varepsilon}_{H_i}^{HCS}$ is achieved as in (26).

APPENDIX C

PROOF OF THEOREM 2

From (12) and (13), the CDF of $\gamma_{L_j}^{x_{L_j}}$ and $\gamma_{L_j}^{x_{L_j}}$ are respectively given by

$$F_{\gamma_{L_j}^{x_{L_j}}}(x) = \Pr \left\{ \frac{\alpha_{H_i} \gamma_0 g_{SL}}{\alpha_{L_j} \gamma_0 g_{SL} + 1} < x \right\} \quad (56)$$

$$= F_{g_{SL}}(B_x),$$

and

$$F_{\gamma_{L_j}^{x_{L_j}}}(x) = \Pr \left\{ \alpha_{L_j} \gamma_0 g_{SL} < x \right\}$$

$$= F_{g_{SL}} \left(\frac{x}{\alpha_{L_j} \gamma_0} \right). \quad (57)$$

To derive $\bar{\varepsilon}_{L_j}^{HCS}$ in (27), we need to resolve $\bar{\varepsilon}_{L_j}^{x_{H_i}, HCS}$ and $\bar{\varepsilon}_{L_j}^{x_{L_j}, HCS}$. For $\bar{\varepsilon}_{L_j}^{x_{H_i}, HCS}$, from (22), (20), and (56), it can be expressed as

$$\bar{\varepsilon}_{L_j}^{x_{H_i}, HCS} \approx 1 + \chi_{H_i} \sqrt{N_{H_i}} \sum_{p=1}^{a_{L,i}} \sum_{\Delta_L=p} \Phi_{LCL,I}$$

$$\times \int_{v_{H_i}}^{\mu_{H_i}} B_x^{\varphi_L} e^{-\frac{p m_L B_x}{\lambda_{SL}}} dx. \quad (58)$$

After some algebraic manipulations similar to the proof of Theorem 1 in Appendix B, the final expression for $\bar{\varepsilon}_{L_j}^{x_{H_i}, HCS}$ can be obtained as in (27).

For $\bar{\varepsilon}_{L_j}^{x_{L_j}, HCS}$, we derive it with the aid of (20), (22), and (57) as follows:

$$\bar{\varepsilon}_{L_j}^{x_{L_j}, HCS} \approx 1 + \chi_{L_j} \sqrt{N_{L_j}} \sum_{p=1}^{a_{L,i}} \sum_{\Delta_L=p} \frac{\Phi_{LCL,I}}{(\alpha_{L_j} \gamma_0)^{\varphi_L}}$$

$$\times \int_{v_{L_j}}^{\mu_{L_j}} x^{\varphi_L} e^{-\hat{\omega}_L x} dx. \quad (59)$$

By using [41, Eq. (3.351.2)], the integral in (59) can be represented as

$$\int_{v_{L_j}}^{\mu_{L_j}} x^{\varphi_L} e^{-\hat{\omega}_L x} dx = \hat{\omega}_L^{-\varphi_L - 1} \Xi_{L,4}, \quad (60)$$

where $\Xi_{L,4}$ is defined in (27). By substituting (60) into (59), we obtain the final expression for $\bar{\varepsilon}_{L_j}^{x_{L_j}, HCS}$ as in (27).

REFERENCES

- [1] H. Ji, S. Park, J. Yeo, Y. Kim, J. Lee, and B. Shim, "Ultra-reliable and low-latency communications in 5G downlink: Physical layer aspects," *IEEE Wireless Commun.*, vol. 25, no. 3, pp. 124–130, Jun. 2018.
- [2] P. Popovski, J. J. Nielsen, C. Stefanovic, E. de Carvalho, E. Strom, K. F. Trillingsgaard, A.-S. Bana, D. M. Kim, R. Kotaba, J. Park, and R. B. Sorensen, "Wireless access for ultra-reliable low-latency communication: Principles and building blocks," *IEEE Netw.*, vol. 32, no. 2, pp. 16–23, Mar. 2018.
- [3] S. K. Sharma and X. Wang, "Toward massive machine type communications in ultra-dense cellular IoT networks: Current issues and machine learning-assisted solutions," *IEEE Commun. Surveys Tuts.*, vol. 22, no. 1, pp. 426–471, Firstquarter 2020.
- [4] G. J. Sutton, J. Zeng, R. P. Liu, W. Ni, D. N. Nguyen, B. A. Jayawickrama, X. Huang, M. Abolhasan, Z. Zhang, E. Dutkiewicz, and T. Lv, "Enabling technologies for ultra-reliable and low latency communications: From PHY and MAC layer perspectives," *IEEE Commun. Surveys Tuts.*, vol. 21, no. 3, pp. 2488–2524, Feb. 2019.
- [5] G. Durisi, T. Koch, and P. Popovski, "Toward massive, ultrareliable, and low-latency wireless communication with short packets," *Proc. IEEE*, vol. 104, no. 9, pp. 1711–1726, Sep. 2016.

- [6] Y. Polyanskiy, H. V. Poor, and S. Verdú, "Channel coding rate in the finite blocklength regime," *IEEE Trans. Inf. Theory*, vol. 56, no. 5, pp. 2307–2359, May 2010.
- [7] W. Yang, G. Durisi, T. Koch, and Y. Polyanskiy, "Quasi-static multiple-antenna fading channels at finite blocklength," *IEEE Trans. Inf. Theory*, vol. 60, no. 7, pp. 4232–4265, Jun. 2014.
- [8] M. Mousaei and B. Smida, "Optimizing pilot overhead for ultra-reliable short-packet transmission," in *IEEE Int. Conf. Commun. (ICC)*, Paris, France, May 2017.
- [9] L. Dai, B. Wang, Y. Yuan, S. Han, C.-L. I, and Z. Wang, "Nonorthogonal multiple access for 5G: Solutions, challenges, opportunities, and future research trends," *IEEE Commun. Mag.*, vol. 53, no. 9, pp. 74–81, Sep. 2015.
- [10] L. Lei, L. You, Y. Yang, D. Yuan, S. Chatzinotas, and B. Ottersten, "Load coupling and energy optimization in multi-cell and multi-carrier NOMA networks," *IEEE Trans. Veh. Technol.*, vol. 68, no. 11, pp. 11 323–11 337, Nov. 2019.
- [11] L. Dai, B. Wang, Z. Ding, Z. Wang, S. Chen, and L. Hanzo, "A survey of non-orthogonal multiple access for 5G," *IEEE Commun. Surveys Tuts.*, vol. 20, no. 3, pp. 2294–2323, Thirdquarter 2018.
- [12] A. C. Cirik, N. M. Balasubramanya, L. Lampe, G. Vos, and S. Bennett, "Toward the standardization of grant-free operation and the associated NOMA strategies in 3GPP," *IEEE Commun. Stand. Mag.*, vol. 3, no. 4, pp. 60–66, Dec. 2019.
- [13] 3rd Generation Partnership Project (3GPP), "Study on downlink multiuser superposition transmission (MUST) for LTE," 3GPP, Tech. Rep. 36.859, Jan. 2016.
- [14] —, "Evolved universal terrestrial radio access (E-UTRA); Physical channels and modulation," 3GPP, Tech. Rep. TS 36.211, Apr. 2020.
- [15] —, "Study on non-orthogonal multiple access (NOMA) for NR," 3GPP, Tech. Rep. 38.812, Dec. 2018.
- [16] X. Sun, S. Yan, N. Yang, Z. Ding, C. Shen, and Z. Zhong, "Short-packet downlink transmission with non-orthogonal multiple access," *IEEE Trans. Wireless Commun.*, vol. 17, no. 7, pp. 4550–4564, Jul. 2018.
- [17] B. Makki, K. Chitti, A. Behravan, and M.-S. Alouini, "A survey of NOMA: Current status and open research challenges," *IEEE Open J. Commun. Soc.*, no. 1, pp. 179–189, Jan. 2020.
- [18] I. Budhiraja, N. Kumar, and S. Tyagi, "Cross-layer interference management scheme for D2D mobile users using NOMA," *IEEE Syst. J.*, pp. 1–12, Jun. 2020, Early Access.
- [19] Z. Chang, L. Lei, H. Zhang, T. Ristaniemi, S. Chatzinotas, B. Ottersten, and Z. Han, "Secure and energy-efficient resource allocation for multiple-antenna NOMA with wireless power transfer," *IEEE Trans. Green Commun. Netw.*, vol. 2, no. 4, pp. 1059–1071, Dec. 2018.
- [20] Q. Yu, C. Han, L. Bai, J. Wang, J. Choi, and X. Shen, "Multiuser selection criteria for MIMO-NOMA systems with different detectors," *IEEE Trans. Veh. Technol.*, vol. 69, no. 2, pp. 1777–1791, Feb. 2020.
- [21] M. Zeng, A. Yadav, O. A. Dobre, G. I. Tsiropoulos, and H. V. Poor, "Capacity comparison between MIMO-NOMA and MIMO-OMA with multiple users in a cluster," *IEEE J. Sel. Areas Commun.*, vol. 35, no. 10, pp. 2413–2424, Oct. 2017.
- [22] Y. Yu, H. Chen, Y. Li, Z. Ding, and L. Zhuo, "Antenna selection in MIMO cognitive radio-inspired NOMA systems," *IEEE Commun. Lett.*, vol. 21, no. 12, pp. 2658–2661, Dec. 2017.
- [23] Y. Yu, H. Chen, Y. Li, Z. Ding, L. Song, and B. Vucetic, "Antenna selection for MIMO nonorthogonal multiple access systems," *IEEE Trans. Veh. Technol.*, vol. 67, no. 4, pp. 3158–3171, Apr. 2018.
- [24] Y. Yu, H. Chen, Y. Li, Z. Ding, and B. Vucetic, "On the performance of non-orthogonal multiple access in short-packet communications," *IEEE Commun. Lett.*, vol. 22, no. 3, pp. 590–593, Mar. 2018.
- [25] J. Zheng, Q. Zhang, and J. Qin, "Average block error rate of downlink NOMA short-packet communication systems in nakagami-m fading channels," *IEEE Commun. Lett.*, vol. 23, no. 10, pp. 1712–1716, Oct. 2019.
- [26] X. Lai, Q. Zhang, and J. Qin, "Cooperative NOMA short-packet communications in flat Rayleigh fading channels," *IEEE Trans. Veh. Technol.*, vol. 68, no. 6, pp. 6182–6186, Jun. 2019.
- [27] Z. Wang, T. Lv, Z. Lin, J. Zeng, and P. T. Mathiopoulos, "Outage performance of URLLC NOMA systems with wireless power transfer," *IEEE Wireless Commun. Lett.*, vol. 9, no. 3, pp. 380–384, Mar. 2020.
- [28] C. Xiao, J. Zeng, W. Ni, X. Su, R. P. Liu, T. Lv, and J. Wang, "Downlink MIMO-NOMA for ultra-reliable low-latency communications," *IEEE J. Sel. Areas Commun.*, vol. 37, no. 4, pp. 780–794, Apr. 2019.
- [29] X. Huang and N. Yang, "On the block error performance of short-packet non-orthogonal multiple access systems," in *IEEE Int. Conf. Commun. (ICC)*, Shanghai, China, May 2019.
- [30] N. Yang, P. L. Yeoh, M. Elkashlan, R. Schober, and I. B. Collings, "Transmit antenna selection for security enhancement in MIMO wiretap channels," *IEEE Trans. Commun.*, vol. 61, no. 1, pp. 144–154, Jan. 2013.
- [31] T. N. Do, D. B. d. Costa, T. Q. Duong, and B. An, "Improving the performance of cell-edge users in MISO-NOMA systems using TAS and SWIPT-based cooperative transmissions," *IEEE Trans. Green Commun. Netw.*, vol. 2, no. 1, pp. 49–62, Mar. 2018.
- [32] Z. Ding, L. Dai, and H. V. Poor, "MIMO-NOMA design for small packet transmission in the internet of things," *IEEE Access*, vol. 4, pp. 1393–1405, Apr. 2016.
- [33] Z. Ding, H. Dai, and H. V. Poor, "Relay selection for cooperative NOMA," *IEEE Wireless Commun. Lett.*, vol. 5, no. 4, pp. 416–419, Jun. 2016.
- [34] D.-D. Tran, D.-B. Ha, V. N. Vo, C. So-In, H. Tran, T. G. Nguyen, Z. A. Baig, and S. Sanguanpong, "Performance analysis of DF/AF cooperative MISO wireless sensor networks with NOMA and SWIPT over Nakagami-m fading," *IEEE Access*, vol. 6, pp. 56 142–56 161, Oct. 2018.
- [35] Z. Ding, P. Fan, and H. V. Poor, "Impact of user pairing on 5G nonorthogonal multiple access downlink transmissions," *IEEE Trans. Veh. Technol.*, vol. 65, no. 8, pp. 6010–6023, Aug. 2016.
- [36] Y. Liu, Z. Ding, M. Elkashlan, and H. V. Poor, "Cooperative nonorthogonal multiple access with simultaneous wireless information and power transfer," *IEEE J. Sel. Areas Commun.*, vol. 34, no. 4, pp. 938–953, Apr. 2016.
- [37] J. Wang, B. Xia, K. Xiao, and Z. Chen, "Performance analysis and power allocation strategy for downlink NOMA systems in large-scale cellular networks," *IEEE Trans. Veh. Technol.*, vol. 69, no. 3, pp. 3459–3464, Mar. 2020.
- [38] D. C. González, D. B. da Costa, and J. C. S. S. Filho, "Distributed TAS/MRC and TAS/SC schemes for fixed-gain AF systems with multi-antenna relay: Outage performance," *IEEE Trans. Wireless Commun.*, vol. 15, no. 6, pp. 4380–4392, Jun. 2016.
- [39] B. Makki, T. Svensson, and M. Zorzi, "Finite block-length analysis of the incremental redundancy HARQ," *IEEE Wireless Commun. Lett.*, vol. 3, no. 5, pp. 529–532, Oct. 2014.
- [40] X. Zhang, X. Zhou, and M. R. McKay, "Enhancing secrecy with multi-antenna transmission in wireless ad hoc networks," *IEEE Trans. Inf. Forensics Security*, vol. 8, no. 11, pp. 1802–1814, Nov. 2013.
- [41] I. Gradshteyn and I. Ryzhik, *Table of Integrals, Series, and Products*, 7th ed. Academic Press, Mar. 2007.